WAKE-BPAT: WAVELET-BASED ADAPTIVE KALMAN FILTERING FOR BLOOD PRESSURE ESTIMATION VIA FUSION OF PULSE ARRIVAL TIMES

Golnar Kalantar[†], *Sourav K. Mukhopadhyay*[⊤], *Fatemeh Marefat*[‡], *Pedram Mohseni*[‡], *Arash Mohammadi*[†]

[†] Concordia Institute for Information System Engineering, Concordia University, Montreal, Canada
[⊤] Electrical and Computer Engineering, Concordia University, Montreal, Canada
[‡] Electrical Engineering and Computer Science, Case Western Reserve University, Cleveland, OH, USA
Emails:{g_kalant, arashmoh, s_mukho}@encs.concordia.ca,{fatemeh.marefat, pedram.mohseni}@case.edu

ABSTRACT

The paper is motivated by recent urgency to design continuous and cuff-less blood pressure (BP) monitoring solutions to prevent, detect, and treat the hypertension. In this regard, we propose a novel wavelet-based feature extraction algorithm coupled with an adaptive and multiple-model Kalman filtering framework (referred to as the WAKE-BPAT), which provides accurate and dynamic BP estimates by extraction and fusion of ***different pulse arrival time (PAT)*** features. In particular, a wavelet transform and histogram analysis-based robust and high-accurate R-peak detection algorithm is proposed without incorporation of any pre-defined thresholds. This in combination with high-quality photoplethysmogram (PPG) characteristic points obtained from signal recordings of a recently developed PPG device (Gen-1), are used for BP estimation, which is modeled as a hybrid state-space model with structural uncertainties to fuse different PAT features in an adaptive fashion. Our experimental evaluations based on a real data set collected via Gen-1 device confirms the superiority of the proposed WAKE-BPAT framework in comparison to its counterparts.

Index Terms— Blood Pressure Estimation, Photoplethysmogram, Pulse Arrival Time, Wavelet Transform, Kalman Filter.

1. INTRODUCTION

Blood pressure (BP) is a crucial hemodynamic parameter that varies between two pressure levels in each heartbeat, called the Systolic BP (SBP) and the Diastolic BP (DBP). Hypertension, which is also known as High Blood Pressure (HBP), is defined as a medical condition in which arteries are experiencing a persistently elevated blood pressure, and is the cause for at least 45% deaths due to heart disease, and 51% of deaths due to stroke [1]. The HBP is usually referred to as the silent killer, as it does not show up significant symptoms. However, long-term high blood pressure is a principal risk factor for coronary artery disease, stroke, heart failure, peripheral vascular disease, vision loss, and chronic kidney disease [2]. An individual is called Hypertensive, if their SBP or DBP reaches more than 140 or 90 mmHg respectively, at rest [3]. The BP measurements, and in particular, continuous BP measurements are great means of retrieving invaluable information about subjects' health conditions in order to prevent, detect, evaluate, and early start of treatment of hypertension [4]. Conventionally, cuff-based instruments are used to determine the BP, which are by nature discontinuous means of measurement, time consuming to use, and also cause discomfort and inconvenience in case of many repetitions.

The aforementioned drawbacks of cuff-based BP monitoring have resulted in a recent surge of interest [5–13] to develop novel and innovative signal processing solutions for continuous BP monitoring. A potential surrogate of BP which is able to perform BP measurements non-invasively and continuously is the Pulse Arrival Time (PAT), which is defined as the time for the pulse to travel from the heart to a peripheral site. The PAT is considered as a notably practical solution for ambulatory BP monitoring due to being readily acquired by wearable devices. Ahmad *et al.* [14] showed that a significant correlation exists between the BP and the PAT, however, this correlation depends on several parameters, which vary among different individuals. In this paper, we aim to investigate BP estimation through ECG and PPG signals [15], using the PAT method.

To date, there are numerous proposed methods in the literature for detection of QRS-complex and R-peak. Recently, a derivative and adaptive threshold-based algorithm is proposed by Khamis *et al.* in [16] for the detection of QRS complex. A quadratic filter-based ECG enhancement and QRS detection technique is proposed by Phukpattaranont in [17]. However, the detection performance of such methods is reliant on heuristically determined threshold values, that are either static or dynamic in time or frequency domains. Threshold-based detection approaches, however, are not generally suitable and/or applicable, particularly in presence of in-band noises. On the other hand, we utilize the first-generation (Gen-1) device very recently developed by Marefat and Mohseni*et al.* [15] for collecting PPG signals. The Gen-1 device performs minimally invasive, muscle-based recording of the PPG signal in the reflective mode. Finally, different linear [9] and non-linear models [4, 7] have been developed in the literature to estimate the BP from a computed PAT feature. While most of the model-based BP estimations from PAT are static algorithms in nature, recently dynamic BP estimation via Kalman filtering (KF) [8] is proposed, however, fixed/known parameters are used based on a single first-order scalar Markov model and a single extracted PAT feature.

In this paper, we propose a novel wavelet-based feature extraction algorithm coupled with an adaptive and multiple-model Kalman filtering framework (referred to as the WAKE-BPAT). As the resulting pattern of the PPG wave obtained from Gen-1 device is of high quality, high signal-to-noise ratio (SNR), and is smooth, a derivative and threshold-based technique is developed for extraction of main features from the PPG signals in the WAKE-BPAT framework. Due to incorporation of state-of-the-art PPG recording system (Gen-1 device [15]), performance of continuous and automated BP-measurement relies heavily upon the accuracy of the feature extraction algorithm from ECG signal. A Wavelet Transform (WT) and histogram analysis-based robust and highly-accurate R-peak detection algorithm is proposed here. The novelty of the algorithm lies in its accuracy and simplicity. The algorithm does not use any threshold value for the detection of R-peaks. The third contribution of the paper is development of a novel adaptive, and multiple model [18] KF framework for BP estimation, which considers inherit structural uncertainties of the state and observation models, and fuses different PAT features in an adaptive fashion.

The rest of the paper is organized as follows: Section 2 formulates the problem. The proposed WAKE-BPAT framework is developed in Section 3. Section 4 presents the experimental results. Finally, Section 5 concludes the paper.

2. PROBLEM FORMULATION

As stated previously, the PAT is, typically, derived from ECG and PPG signals. The PPG is a non-invasive measurement technique that measures relative blood volume changes in the blood vessels. On the other hand, the ECG is the graphical representation of the heart's electrical activity, and the QRS-complex (Q, R and S waves are usually treated as a single composite wave known as the QRS-complex) is the most prominent feature of the ECG signal. It provides useful information about the depolarization of ventricular myocardium and indicates the start of ventricular contraction of the heart.

Commonly, the PAT is computed from the time interval between the R-peak of the ECG signal and a characteristic point of the PPG signal. Different features (characteristics points) can be extracted from the PPG signals among which the following three are typically used: (i) The on-set of the PPG; (ii) The peak of the PPG, and; (iii)The peak of the derivative of each PPG cycle i.e, the maximum-slope-point (MSP) of each PPG cycle. Once characteristic points are identified through feature extraction on both the ECG and PPG signals, the next step is to estimate the BP based on the extracted features. The BP estimation task depends on the model used to relate the BP to the selected time difference such as the following

$$\text{Model 1:} \qquad \text{BP} = \alpha_1 \ln(\text{PAT}) + \beta_1 \tag{1}$$

$$\text{Model 2:} \qquad \text{BP} = \alpha_2 \text{PAT} + \beta_2 \tag{2}$$

$$\text{Model 3:} \qquad \text{BP} = \frac{\alpha_3}{\text{PAT}^2} + \beta_3, \tag{3}$$

where the model parameters are, typically, computed through a calibration step, which is performed based on couple of ground truth points and using least square (LS) approach.

We develop a KF-based algorithm for dynamical estimation of the BP values from PAT features. In this context, recently Reference [8] proposed a KF formulation where the BP constitutes the state variable and a simple random walk process is used to model BP dynamics. The observation model is constructed based on a single PAT feature resulting in the following state-space model to track the BP continuously

$$\text{State Model:} \qquad \text{BP}(k) = \text{BP}(k-1) + w(k) \tag{4}$$

$$\text{Observation Model:} \qquad \ln \text{PAT}(k) = \frac{1}{\alpha_1}\text{BP}(k) - \frac{\beta_1}{\alpha_1} + v(k), \tag{5}$$

where k denotes the time index, and $w(k) \sim \mathcal{N}(0, Q)$ and $v(k) \sim \mathcal{N}(0, R)$ represent the forcing terms and the observation noise, respectively. This completes a brief overview of the problem at hand. Next, we present the proposed WAKE-BPAT framework.

3. PROPOSED WAKE-BPAT

The proposed WAKE-BPAT framework consists of three main components namely: (i) Pre-processing; (ii) Feature extraction, and; (iii) BP estimation mechanism. Below, we describe the above mentioned components respectively and in details.

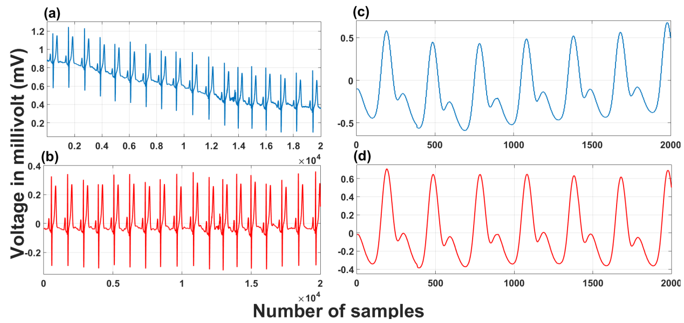

Fig. 1. (a) Noisy ECG signal. (b) Denoised ECG signal. (c) Noisy PPG signal. (d) Denoised PPG signal.

3.1. Pre-processing

At the time of acquisition, ECG signal often gets heavily contaminated by various high and low-frequency noises including the 50/60 Hz power line interference, electrosurgical noise, and baseline drift, which degrades the performance and the accuracy of automated ECG processing algorithms. Therefore, at first, the ECG signal has to be extracted from the background noise. The WT is a well-regarded technique which is able to effectively decompose a signal at various time-frequency resolutions and consequently, WT has been widely utilized for analyzing non-stationary signals such as the ECG.

The ECG signal is characterized by a periodic or quasi-periodic occurrence of various waves and segments having different frequency bands. Hence, WT is considered to be an excellent means for the analysis of ECG signals [19]. Assorted ECG-waves, segments, and also the noises come to be prominent at different frequency bands once subjected to the multi-resolution wavelet analysis. The discrete wavelet transform (DWT)-based ECG de-noising technique used in [20] is adopted in this paper. The clinical bandwidth of ECG signal lies between 0.05-100 Hz [21], and the signal is recorded at various sampling rates starting from 200Hz. To bring uniformity to the processing approach of ECG signals recorded at different sampling rates, the signal is re-sampled at 1KHz, and then the signal is decomposed using DWT by selecting the Biorthogonal 6.8 wavelet (bior6.8) as the mother wavelet function.

High and low-frequency noises are eliminated by discarding the corresponding detail and approximation wavelet-coefficients from the noisy signal. On the other hand, all the clinical signatures of PPG signal reside below 25 Hz [22], and therefore, the PPG signal is recorded at different sampling rates starting from 50Hz. Hence, the input PPG signal is also re-sampled at 1 KHz due to the same reason as in the case of ECG. The DWT-based signal denoising technique, which has been used for ECG is also used for PPG, selecting the 'db8' wavelet function from the Daubechie's wavelet family [7]. An illustration of noisy and denoised ECG and PPG signals are shown in Fig 1.

3.2. Feature Extraction

The feature extraction component of the proposed WAKE-BPAT framework consists of two main tasks as explained below.

3.2.1. The R-peak Detection

Since the detail-coefficients *D4* and *D5* of the wavelet transformed data contain most of the information-energy of the QRS-

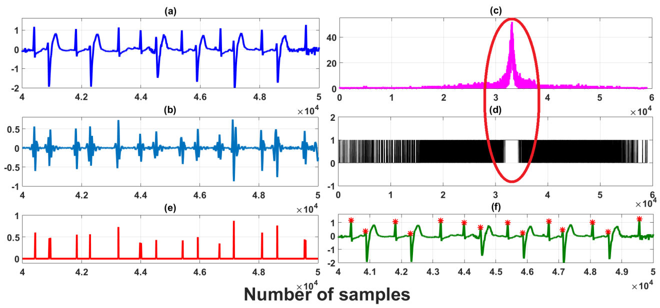

Fig. 2. (a) Denoised ECG. (b) *QRS-coef* data. (c) Histogram analysis of the *QRS-coef*. (d) Amplitude-band where the population of coefficients is maximum. (e) Modified *QRS-coef* data. (f) Detected R-peaks.

complex [20], these two coefficient-bands are selected for the purpose of R-peak detection. An array, which is denoted as *QRS-coef* is formed by adding the coefficients of the *D4* and *D5* (*QRS-coef* = *D4* + *D5*). The local peaks of the data present in the *QRS-coef* array clearly indicate the QRS-complexes of the denoised signal. To eliminate the contribution of other waves and segments on the *QRS-coef* data, and to boost the detection accuracy of the R-peak points, histogram analysis of the wavelet coefficients present in the *QRS-coef* array is performed. Since most of the samples of an ECG-beat (one complete ECG cycle is considered as a beat) belong to the low-frequency non-QRS regions (T and P-peaks, ST-segment etc.), the peak of the histogram, and its surrounding samples values constitute the non-QRS regions. The amplitude-band where the population of coefficients is maximum is identified from the histogram analysis, and the corresponding amplitudes of those coefficients are made zero in the *QRS-coef* array. Finally, the local peaks are identified from the modified *QRS-coef* array, and the corresponding indices are marked as R-peak in the filtered signal. Figure 2 demonstrates the fact. The R-peak detection algorithm has been tested on a large number of ECG data files of different sampling rates, and the accuracy is found over 99.9%.

3.2.2. Fiducial-point Detection from PPG Signal

First-derivative of the filtered PPG (FD-PPG) signal is calculated, and two different features are extracted from the FD-PPG signal: (1) maximum-slope-point (MSP) of every PPG cycle, and (2) systolic-peaks. The maximum amplitude of the FD-PPG signal is found, and the indexes of those samples having an amplitude within 25% of the maximum are marked, and then the local-maximum amplitude within a sliding-window of width 0.25s [23] is identified and considered as the MSP of that PPG cycle. Now, traversing right in the time-domain PPG signal from the most recently detected MSP, the first slope-reversal event is identified as the systolic-peak. Figure 3 demonstrates the operations.

Now, the PPG-onset point is detected using a different method. First, the systolic-peak intervals in the filtered signal are divided into 2:1 ratio, i.e., the mid-point of the peak-to-peak interval is calculated, which is denoted as "M". Then, all the samples in between every M-point and the immediate next MSP are considered. Thereafter, among those considered samples, the maximum value of angle θ is found, and the corresponding index on the filtered PPG is marked as the PPG-onset point. Figure 4(a) shows the operations, while Figure 4(b) illustrates the Gen-1 Device.

3.3. BP Estimation Models

We developed an adaptive KF-based algorithm for dynamical esti-

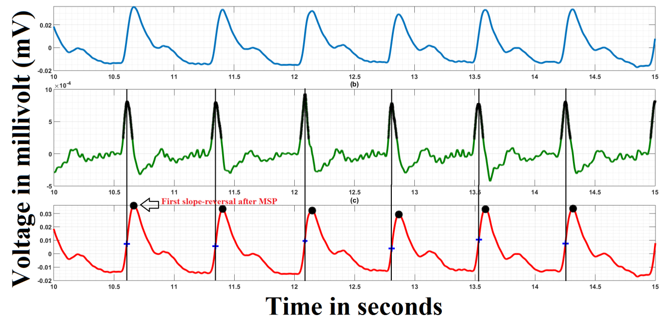

Fig. 3. (a) Filtered PPG. (b) FD-PPG signal where marked samples are the ones within the threshold value. (c) Detected MSP and systolic-peaks.

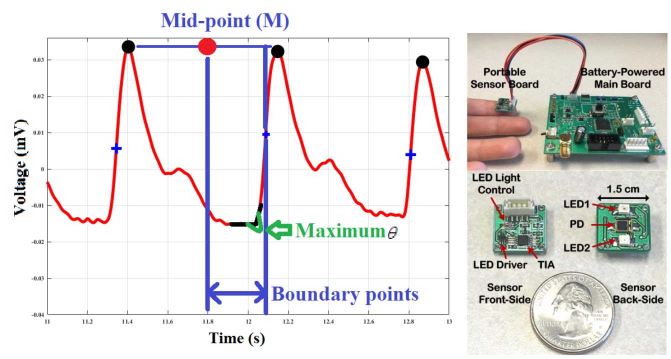

(a) (b)

Fig. 4. (a) The PPG-onset detection technique. (b) The Gen-1 Device for PPG recordings developed recently by Marefat and Mohseni*et al.* [15].

mation of the BP values from features extracted in Section 3.2. Unlike the conventional approach of using a simple random walk to model BP evolutions over time, we use an Autoregressive (AR) process of order p (in the experiments we used $p = 4$) for relating the current BP estimates to its previous ($N > 1$) values, i.e.,

$$\mathrm{BP}(k) = \sum_{i=1}^{p} a_i(k)\mathrm{BP}(k-i) + w(k), \tag{6}$$

where a_i, for ($1 \leq i \leq p$), denotes the AR coefficients to be updated at each iteration. The evolution of the AR coefficients is modeled as

$$\boldsymbol{a}(k) \triangleq [a_1(k), \ldots, a_p(k)]^T = \boldsymbol{a}(k-1) + \boldsymbol{\nu}(k), \tag{7}$$

where superscript T denotes transpose operator, and $\boldsymbol{\nu}(k)$ is considered to follow a zero-mean and white Gaussian process with known covariance matrix. To recursively update the AR coefficients, we run a KF based on Reference [24] where an instantaneous (static) estimate of the current BP based on Model 3 in Eq. (3) is used in the update step of the KF implemented for updating the AR coefficients.

Instead of using a single observation model (such as the one introduced in Eq. (5)), we propose to use a bank (combination) of ($N_f > 1$) different observation models and construct a hybrid state-space model for recursive estimation of the BP (in the experiments we used $N_f = 2$ based on the two characteristic points of the PAT features). In other words, we propose to consider a combination of observation models (PAT features) and fuse the estimation result based on each feature using adaptively computed weights. Intuitively speaking, the reason behind this scenario is that one feature might

Table 1. Estimated BP versus the actual BP based on the proposed WAKE-BPAT.

Statistics	WAKE-BPAT	Proposed Features via Model 1	Reference [12]	Reference [10]
Mean Error	**2.67**	3.47	4.32	4.46
Standard Deviation	**2.51**	2.79	5.46	6.05
RMSE	**3.62**	4.41	5.52	5.74

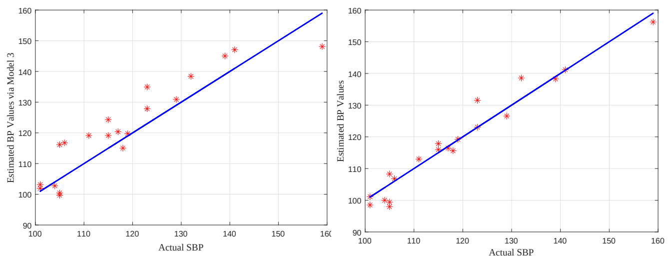

(a) (b)

Fig. 5. Estimated versus the actual BP. (a) Based on [12], i.e., Model 3. (b) Based on the proposed WAKE-BPAT and Model 1.

not be the best choice at all times and potentially using different measurement models would improve the performance. The observation model used in the WAKE-BPAT is, therefore, given by

$$y^{(l)}(k) = C_1^{(l)}\text{BP}(k) + C_2^{(l)} + v^{(l)}(k), \tag{8}$$

where superscript l, for $(1 \leq l \leq N_f)$, refers to one of the candidate PAT features/models within the set of N_f considered multiple models, and $y^{(l)}(k)$ denotes its associated PAT measurement. For example, when Model 1 in Eq. (1) is included in the set of candidate models, the mode-matched terms in Eq. (8) are defined based on Eq. (5) as follows: $y^{(l)}(k) \triangleq \ln \text{PAT}(k)$, $C_1^{(l)} \triangleq \frac{1}{\alpha_1}$, and $C_2^{(l)} \triangleq -\frac{\beta_1}{\alpha_1}$. A KF is matched to each observation model l to form an updated BP estimate defined as $\hat{\text{BP}}^{(l)}(k) \triangleq \mathbb{E}\{\text{BP}(k)|\boldsymbol{Y}^{(l)}(k)\}$ where $\boldsymbol{Y}^{(l)}(k) = \{y^{(l)}(1), \ldots, y^{(l)}(k)\}$ is the set of all available observations upto and including the current iteration, and $\mathbb{E}\{\cdot\}$ denotes expectation operator. The mode-matched KFs are then fused through a collapsing step [18] which forms the optimal single Gaussian distribution in the mean-square error (MSE). Details of adaptive multiple model KF estimation is not included here due to lack of space, please refer to [18] and references therein for further details.

4. SIMULATION AND RESULTS

In this section, we present experimental results based on a real data set collected from a healthy female volunteer. The BP variation is introduced by change in posture and exercise of the volunteer. The measured BP varied between 101 to 159 mmHg. The ECG signals are collected via a 3-lead ECG commercial device, while the PPG recordings are collected based on the Gen-1 device from fingertip. As stated previously, Gen-1 device is very recently developed by Marefat and Mohseni *et al.*, which records the PPG signals in the reflective mode using a portable sensor board interfaced with a battery-powered main board for control and data processing. Please refer to Reference [15] for further details on the Gen-1 device. Finally, 20 reference BP recordings are measured by a cuff-based Omron 10 device. The results obtained based on all 20 measurements with Point 5 with BP equal to 101 mmHg, and Point 6 with BP equal to 141 mmHg are used for calibration via the LS approach. The PAT values are averaged over previous 10 epochs at each ground truth point. Four different BP estimation algorithms are implemented and compared for accuracy as follows: (i) The proposed WAKE-BPAT framework which provides dynamical estimates of the BP and uses the proposed features together with the proposed adaptive and multiple model KF; (ii) Instantaneous (static) BP estimation based on Model 1 and the proposed features; (iii) Instantaneous BP estimation based on [12], and; (iv) Instantaneous BP estimation based on [10].

Table 1, compares the accuracy of the above four estimation algorithms in terms of the mean error in absolute value, the standard deviation, and the root mean squared error (RMSE). It is worth mentioning that mean estimation error below 5 mmHg (in absolute value) with standard derivation of below 8 mmHg is the requirement set by the Association for the Advancement of Medical Instrumentation. It is observed that the proposed WAKE-BPAT framework provides significantly superior results in comparison to its counterpart based on previously developed features. In particular, the mean error in absolute value is reduced approximately in half. At the same time, the effect of the proposed feature extraction algorithms is observed in the improved accuracy of Item (ii). This improvement can be attributed to the proposed histogram analysis of the wavelet coefficients, which not only helps removing the contribution of other waves, but also the presence of in-band noises, which in-turns serves to accurately and reliably detect R-peaks. The prime advantage of the proposed R-peak detection algorithm over others is that it does not require any threshold value for the estimation of the peaks. This algorithm is also potential to be effectively employed in a variety of applications including heart rate calculation, heart rate variability estimation, and classification of ECG beats. Fig. 5 compares the estimation error results in absolute value versus the actual BP values computed based on Items (i) and (iii). It is observed the proposed WAKE-BPAT framework outperforms its counterpart and the estimated BP values are fairly close to their actual ground truth, which attests to the effectiveness of the proposed cuff-less and continuous BP estimation framework.

5. CONCLUSION

In this paper, we proposed a novel framework for non-invasive and continuous estimation of the blood pressure (BP) from Pulse Arrival Time (PAT). The PAT is computed from the time interval between the R-peak of the ECG signal and a characteristic point of the PPG signal collected based on a recently developed PPG recording device (Gen-1). In particular, we proposed a wavelet-based feature extraction algorithm coupled with an adaptive and multiple-model Kalman filtering framework (referred to as the WAKE-BPAT), which provides accurate BP estimates by extraction/fusion of different PAT characteristics. The proposed WAKE-BPAT framework is evaluated based on a real data set, and it was shown that the proposed framework significantly outperforms its counterparts. One potential venue for future investigation is to use nonlinear filters instead of the KF.

6. REFERENCES

[1] "A Global Brief on Hypertension: Silent Killer, Global Public Health Crisis", *World Health Organization*, Geneva, Switzerland, 2014.

[2] D.T. Lackland and M.A. Weber "Global Burden of Cardiovascular Disease and Stroke: Hypertension at the Core," *Canadian Journal of Cardiology*, 31(5), pp. 569-571, 2015.

[3] World Health Organization, "World Health Statistics 2015," *World Health Organization*, 2015.

[4] X. R. Ding, Y. T. Zhang, J. Liu, W. X. Dai, and H. K. Tsang, "Continuous Cuffless Blood Pressure Estimation using Pulse Transit Time and Photoplethysmogram intensity Ratio," *IEEE Transactions on Biomedical Engineering*, vol. 63, no. 5, 964-972, 2016.

[5] T.M. Seeberg *et al.*, "A Novel Method for Continuous, Non-invasive, Cuff-Less Measurement of Blood Pressure: Evaluation in Patients With Nonalcoholic Fatty Liver Disease," *IEEE Transactions on Biomedical Engineering*, vol. 64, no. 7, pp. 1469-1478, 2017.

[6] M. Gao, H.M. Cheng, S.H. Sung, C.H. Chen, N.B. Olivier and R. Mukkamala, "Estimation of Pulse Transit Time as a Function of Blood Pressure Using a Nonlinear Arterial Tube-Load Model," *IEEE Transactions on Biomedical Engineering*, vol. 64, no. 7, pp. 1524-1534, 2017.

[7] M. Kachuee, M. M. Kiani, H. Mohammadzade, and M. Shabany, "Cuffless Blood Pressure Estimation Algorithms for Continuous Health-Care Monitoring," *IEEE Transactions on Biomedical Engineering*, vol. 64, no. 4, pp. 859-869, 2017.

[8] Q. Zhang *et al.* "Cuff-less Blood Pressure Measurement using Pulse Arrival Time and a Kalman Filter," *J. Micromech. Microeng.*, vol. 27, 2017.

[9] R. Mukkamala *et al.*, "Toward Ubiquitous Blood Pressure Monitoring via Pulse Transit Time: Theory and Practice," *IEEE Transactions on Biomedical Engineering*, vol. 62, no. 8, pp. 1879-1901, 2015.

[10] Y.L. Zheng, B.P. Yan, Y.T. Zhang and C.C.Y. Poon, "An Armband Wearable Device for Overnight and Cuff-Less Blood Pressure Measurement," *IEEE Transactions on Biomedical Engineering*, vol. 61, no. 7, pp. 2179-2186, 2014.

[11] V. Chandrasekaran, R. Dantu, S. Jonnada, S. Thiyagaraja, and K. P. Subbu, "Cuffless Differential Blood Pressure Estimation using Smart Phones," *IEEE Transactions on Biomedical Engineering*, vol. 60, no. 4, pp. 1080-1089, 2013.

[12] M. Theodor *et al.* "Subcutaneous Blood Pressure Monitoring with an Implantable Optical Sensor," *Biomedical Microdevices*, vol. 15, no.5, pp. 811-820, 2013.

[13] Y. Chen, C. Wen, G. Tao, M. Bi, and G. Li, "Continuous and Noninvasive Blood Pressure Measurement: A Novel Modeling Methodology of the Relationship Between Blood Pressure and Pulse Wave Velocity," *Annals of Biomedical Engineering*, vol. 37, no. 11, pp. 2222-2233, 2009.

[14] S. Ahmad, S. Chen, K. Soueidan, I. Batkin, M. Bolic, H. Dajani, and V. Groza, "Electrocardiogram-assisted Blood Pressure Estimation," *IEEE Transactions on Biomedical Engineering*, vol. 59, no. 3, pp. 608-618, 2012.

[15] F. Marefat, R. Erfani, K. L. Kilgore and P. Mohseni, "Minimally Invasive Muscle-based Recording of Photoplethysmogram Toward Chronic Implantation," *IEEE Biomedical Circuits and Systems Conference (BioCAS)*, pp. 388-391, 2016.

[16] H. Khamis, R. Weiss, Y. Xie, C. W. Chang, N. H. Lovell,and S. J. Redmond, "QRS Detection Algorithm for Telehealth Electrocardiogram Recordings," *IEEE Transactions on Biomedical Engineering*, vol. 63, no. 7, pp. 1377-1388, 2016.

[17] P. Phukpattaranont, "QRS Detection Algorithm based on the Quadratic Filter," *Expert Systems with Applications*, 42(11), 4867-4877, 2015.

[18] A. Mohammadi and K. N. Plataniotis, "Improper Complex-Valued Multiple-Model Adaptive Estimation," *IEEE Transactions on Signal Processing*, vol. 63, no. 6, pp. 1528-1542, 2015.

[19] E. B. Mazomenos, D. Biswas, A. Acharyya, T. Chen, K. Maharatna, J. Rosengarten, J. Morgan, and N. Curzen, "A Low-Complexity ECG Feature Extraction Algorithm for Mobile Healthcare Applications," *IEEE Journal of Biomedical and Health Informatics*, vol. 17, no. 2, pp. 459-469, 2013.

[20] S. Banerjee, and M. Mitra, "Application of Cross Wavelet Transform for ECG Pattern Analysis and Classification," *IEEE Transactions on Instrumentation and Measurement*, vol. 63, no. 2, 2014.

[21] W. J. Tompkins, "Biomedical Digital Signal Processing," *New Delhi: Prentice Hall of India Pvt. Ltd*, New Delhi, India, 2006.

[22] S. K. Mukhopadhyay, M. Omair Ahmad, and M.N.S. Swamy, "ASCII-Character-Encoding based PPG Compression for Tele-Monitoring System," *Biomedical Signal Processing and Control*, vol. 31, pp. 470-482, 2017.

[23] S.K. Mukhopadhyay, S. Mitra, M. Mitra, "ECG Feature Extraction Using Differentiation, Hilbert Transform, Variable Threshold and Slope Reversal Approach," *Journal of Medical Engineering and Technology*, vol. 36, no. 7, pp. 372-386, 2012.

[24] M. Arnold, X.H.R. Milner, H. Witte, R. Bauer and C. Braun, "Adaptive AR Modeling of Nonstationary Time Series by Means of Kalman Filtering," *IEEE Transactions on Biomedical Engineering*, vol. 45, no. 5, pp. 553-562, 1998.